Analytical Model for Investigating Low-Speed Sideswipe Collisions

James R. Funk, Joseph M. Cormier and Charles E. Bain
Biodynamic Research Corporation

SAE International™

For permission and licensing requests contact:

SAE Permissions
400 Commonwealth Drive
Warrendale, PA 15096-0001-USA
Email: permissions@sae.org
Fax: 724-772-4891
Tel: 724-772-4028

SAE®

Global Mobility Database®

*All SAE papers, standards, and selected
books are abstracted and indexed in the
Global Mobility Database.*

For multiple print copies contact:

SAE Customer Service
Tel: 877-606-7323 (inside USA and Canada)
Tel: 724-776-4970 (outside USA)
Fax: 724-776-1615
Email: CustomerService@sae.org

Analytical Model for Investigating Low-Speed Sideswipe Collisions

James R. Funk, Joseph M. Cormier and Charles E. Bain
Biodynamic Research Corporation

ABSTRACT

Vehicle dynamics in sideswipe collisions are markedly different from other types of collisions. Sideswipe collisions are characterized by prolonged sliding contact, often with very little structural deformation. An analytical model was developed to investigate the vehicle dynamics of sideswipe collisions. The vehicles were modeled as rigid bodies, and lateral interaction between the vehicles was modeled with a linear elastic spring. This linear spring was meant to represent the combined lateral stiffness of both vehicles before significant crush develops. Longitudinal interaction between the vehicles was modeled as frictional contact. In order to validate the model, seven (7) low speed (3 – 10 kph), shallow angle (15°) sideswipe collisions were staged with instrumented vehicles. These sideswipe collisions were characterized by long contact durations (~ 1 s) and low accelerations (< 0.4 g's). The experimental collisions were also simulated with EDSMAC. EDSMAC overpredicted peak longitudinal vehicle acceleration by an average of 83% and underpredicted the length of contact damage by an average of 50%. In contrast, the linear spring model accurately predicted the peak longitudinal vehicle acceleration (5% error) when the stiffness parameter was tuned to match the length of contact damage. These results suggest that a non-crush-based linear spring model for calculating inter-vehicular force could significantly improve the accuracy of reconstructions of low speed sideswipe collisions compared to existing methods such as SMAC.

INTRODUCTION

Sideswipe collisions have received relatively little attention in the literature, but are recognized as being difficult to analyze. For the purpose of this paper, a sideswipe collision is defined as a collision in which the angle of impact is shallow and vehicle interaction in the longitudinal direction is frictional. Unlike other collision modes in which the interacting surfaces rapidly achieve a common velocity, sideswipes are characterized by prolonged sliding between the contact surfaces. A low velocity sideswipe may result in damage to several body panels of a vehicle in the form of scratches, scuffs, and abrasions, resulting in substantial repair costs.

It is desirable to be able to reconstruct sideswipe collisions based in part on observed vehicle damage. Due to the importance of frictional forces and the need to characterize vehicle properties at low levels of crush, sideswipes are often difficult collisions to analyze with existing methods. The vehicle dynamics of sideswipe collisions were described by Bailey et al. [1], who conducted eleven (11) shallow angle (<30°) vehicle-to-vehicle sideswipe tests at approach speeds varying from 4.5 – 27 kph. In some tests, vehicle sliding contact involved "snagging" of the two interacting surfaces at points in which the contact surface geometry was irregular. Snagging was recognized as a different contact mechanism from sliding. Damage from snagging involved forward or rearward deformation of a structure. Bailey et al. [1] reported long contact durations (1.5 – 2 s) and generally low accelerations (≤ 3 g's in tests without snagging) in their tests. A method for reconstructing sideswipe collisions was not proposed. Levy [2] presented an elegant method for determining impact velocity in sideswipes in which a cycloidal truck tire mark has been imprinted on the side of the struck vehicle. Although useful, this method is only applicable to a small percentage of sideswipe collisions. Woolley [3] modeled sideswipes in the "IMPAC" accident reconstruction computer program as frictional contact along a defined slip plane. SMAC [4] and CRASHEX [5] also incorporate frictional inter-vehicular sliding forces. However, all of these programs calculate inter-vehicular forces from stiffness coefficients based on vehicle crush profiles measured after crash tests. These stiffness coefficients may not be accurate when modeling sideswipe collisions with little or no crush. No crash test data have been presented to evaluate the accuracy of these programs in analyzing collisions that are dominated by inter-vehicular sliding rather than crush.

The only general analytical approach for analyzing sideswipe collisions that has been compared to experimental data was presented by Toor et al. [6]. Toor et al. calculated lateral inter-vehicular force based on damage using vehicle side stiffness coefficients. Longitudinal force was then calculated assuming an inter-vehicular sliding coefficient of friction of 0.6. Average accelerations were calculated based on these forces with additional analysis to determine regions

where tire slippage occurred. The method was subject to the following limitations and assumptions: snagging was not considered, the vehicle was assumed to be a rigid body, all tires were assumed to be steered straight and free rolling, and inward crush and yaw rotations were assumed to be small. Toor et al. [6] reported on fourteen (14) vehicle-to-barrier tests and four (4) vehicle-to-vehicle tests used to validate the analytical method. The vehicle-to-barrier tests were conducted by steering the surface vehicle so that its side would contact a trunk lid mounted to a barrier. Similarly, in the vehicle-to-vehicle tests, the surface vehicle was steered so that its side would contact the bumper of the contact vehicle, which was also fixed to a barrier. Approach speeds varied from 4 – 10 kph. The approach angle was not reported. Toor et al. [6] reported that their method accurately estimated the speed changes in their vehicle tests.

The method proposed by Toor et al. [6] provides a useful starting point for evaluating sideswipe collision severity. However, the accuracy of the method is questionable for two reasons. First, the force calculation employed by Toor et al. [6] relies entirely on stiffness coefficients that are derived primarily from high speed crash tests with substantial crush. There is little or no data to validate the accuracy of the force calculation at the intended low levels of crush (0 – 4 cm) [7]. Second, the method does not take into account the approach angle between the vehicles. The approach angle strongly influences the length of sliding contact damage, which in turn strongly influences the calculated velocity change and acceleration of the vehicles. Therefore, there is a need for a more detailed analytical model to aid in analyzing low-speed sideswipe collisions.

METHODS

ANALYTICAL MODEL

An analytical model was developed specifically to investigate sideswipe collisions and was implemented as a FORTRAN program. The model is similar to SMAC [4] in that it calculates vehicle kinematics utilizing a forward timewise integration of the equations of rigid body motion. However, the model includes a novel non-crush-based method for calculating inter-vehicular force. An impact configuration is assumed in which the front corner of a bullet vehicle strikes the side of a stationary target vehicle at a given closing velocity and approach angle (Figure 1). The bullet and target vehicles were modeled as rectangular rigid bodies having the dimensions, masses, and inertial properties of the subject vehicles.

Assumptions and limitations of the model

The model was subject to the following assumptions and limitations:

- The combined lateral compliance of both vehicles due to bumper and door panel deformation, suspension, tire sidewall stiffness, etc. was lumped into a single force-deflection relationship (eq. 1).

- Longitudinal interaction between the sliding surfaces was assumed to be frictional. The model may not be valid when snagging or substantial inward crush occurs, because that may cause the longitudinal force to exceed the force expected from pure friction (eq. 2).
- All tires on both vehicles were assumed to be steered straight and free rolling with lateral slippage governed by Coulomb friction.
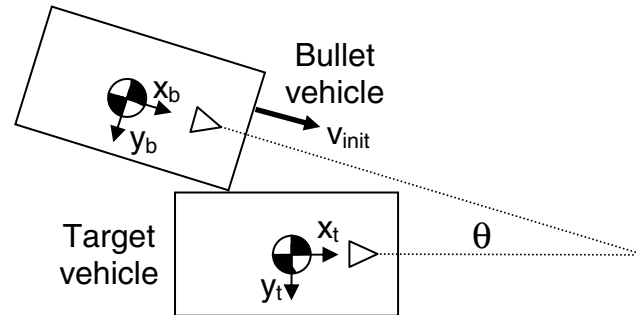

Figure 1. Schematic of vehicle test setup.

Coordinate system

An inertial coordinate frame was established to track the positions of both vehicles. The inertial frame was aligned with the initial position of the target vehicle frame such that its origin was coincident with the center of gravity (CG) of the target vehicle. In accordance with the SAE sign convention, the x-axis pointed forward, the y-axis pointed right, and clockwise rotations were considered positive. The bullet vehicle was assigned an initial position based on its relative approach speed and angle such that its trajectory would cause the bullet vehicle bumper to strike the side of the target vehicle at a predetermined point of initial contact. Equations are presented assuming the right front corner of the forward-moving bullet vehicle strikes the left side of the initially stationary target vehicle. Of course, the equations can be easily manipulated to account for rearward strikes, strikes to the right side of the target vehicle, and initial motion of the target vehicle. As mentioned, vehicle positions were tracked with respect to an inertial coordinate frame. However, vehicle forces, velocities, and accelerations were tracked in the local vehicle coordinate frame originating at the CG of each vehicle (Figure 1). Vehicle velocities were coordinate transformed to the inertial frame before being integrated to obtain positions.

Modeling procedure

Modeling of the vehicle dynamics was performed by solving the equations of motion at a given time point and successively incrementing in time to obtain results over a desired time duration. Because inter-vehicular and tire slip conditions could change the governing equations of motion several times during a simulation, it was necessary to solve the model computationally as an initial value problem. Initial values for all parameters were established at the time in which vehicle contact

initiated. At each subsequent time increment, the following calculations were performed:

1. Vehicle positions were calculated by integrating the vehicle velocity using the trapezoidal rule. Based on the vehicle dimensions, a lateral overlap distance (d_{lat}) was calculated as the perpendicular distance between the side of the target vehicle and the front corner of the bullet vehicle. The longitudinal point of contact was also calculated as the perpendicular distance between the rear axle of the target vehicle and the front corner of the bullet vehicle.

2. The lateral contact force applied to the target vehicle was calculated as a function of the lateral overlap distance (d_{lat}). The force-deflection relationship was modeled as a linear elastic spring:

$$F_{yt} = k \cdot d_{lat} \tag{1}$$

where F_{yt} was the y-axis force applied to the target vehicle and k was the spring stiffness. It is possible to use any force-deflection model, such as a system of nonlinear springs and dashpots, or even an arbitrary function.

3. The longitudinal contact force applied to the target vehicle was calculated assuming frictional contact:

$$F_{xt} = \mu_{slide} \cdot F_{yt} \tag{2}$$

where F_{xt} is the x-axis force applied to the target vehicle and μ_{slide} is the inter-vehicular sliding coefficient of friction. The maximum value for μ_{slide} was assumed to be 0.5. After a common contact velocity was reached, μ_{slide} was calculated to equilibrate the inter-vehicular shear force such that no relative longitudinal acceleration occurred between the bumper of the bullet vehicle and the side of the target vehicle at the contact point. If, later in the event, this calculated shear force exceeded $\pm 0.5 \cdot F_{yt}$, then inter-vehicular sliding resumed.

4. The forces applied to the front corner of the bullet vehicle were calculated from Newton's third law by coordinate transforming the target vehicle forces to the bullet vehicle frame:

$$\begin{bmatrix} F_x \\ F_y \end{bmatrix}_b = \begin{bmatrix} \cos\theta & \sin\theta \\ -\sin\theta & \cos\theta \end{bmatrix} \begin{bmatrix} F_x \\ F_y \end{bmatrix}_t \tag{3}$$

where F_{xb} and F_{yb} were the contact forces applied to the bullet vehicle along its x-axis and y-axis, respectively, and θ was the angle between the vehicles (Figure 2).

5. Once the contact forces were calculated, the front and rear lateral tire forces (F_f and F_r), lateral acceleration (a_y), and angular acceleration (α) were

calculated for each vehicle. Only two dynamic equilibrium equations are available to solve for these four unknowns (Figure 3). These two equations may be obtained by summing the forces in the y-direction and summing the moments about the vehicle CG or the center of the front or rear axle (points f and r in Figure 3). Two additional equations are available if the lateral slip conditions of the tires are known (Table 1). If no tires are slipping laterally, the lateral acceleration and angular acceleration of the vehicle are equal to zero. If the front and/or rear tires are slipping laterally, then the lateral tire force is equal to the maximum available tire force:

$$F_{f\,max} = \mu_{tire} \cdot W \cdot \frac{d_{cg-r}}{d_{wb}} \tag{4a}$$

$$F_{r\,max} = \mu_{tire} \cdot W \cdot \frac{d_{cg-f}}{d_{wb}} \tag{4b}$$

where μ_{tire} is the coefficient of friction between the tires and the ground, W is the weight of the vehicle, d_{cg-r} is the distance from the CG to the rear axle, d_{cg-f} is the distance from the CG to the front axle, and d_{wb} is the wheelbase.
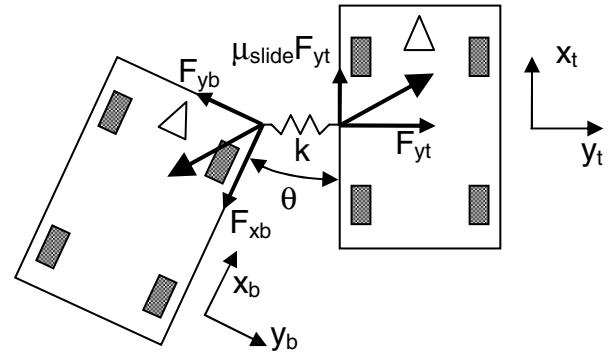

Figure 2. Illustration of the inter-vehicular force interaction. For clarity, negative bullet vehicle forces are shown and the vehicles are drawn separated rather than overlapped.
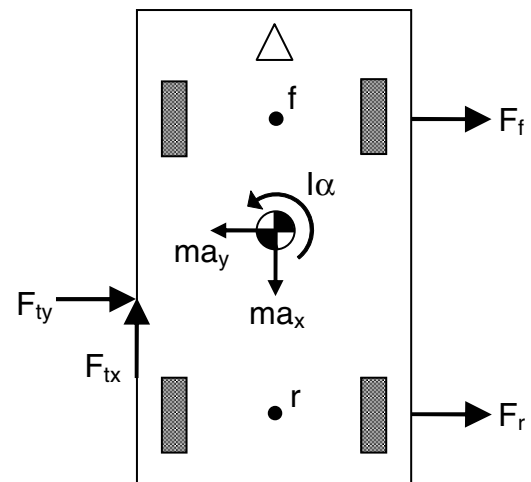

Figure 3. Free body diagram of the target vehicle.

If the front tires are slipping laterally, but the rear tires are gripping, then the lateral acceleration at the CG and the angular acceleration of the vehicle are kinematically related as if the vehicle were rotating about the center of the rear axle:

$$a_y = \alpha \cdot d_{cg-r} \qquad (5a)$$

Similarly, when the rear tires are slipping laterally and the front tires are gripping, then the lateral acceleration at the CG and the angular acceleration of the vehicle are kinematically related as if the vehicle were rotating about the center of the front axle:

$$a_y = \alpha \cdot d_{cg-f} \qquad (5b)$$

Table 1. Governing equations for the vehicle dynamics parameters that depend on the tire slip conditions.

Front tires	Grip	Slip	Grip	Slip
Rear tires	Grip	Grip	Slip	Slip
a_y	0	$\alpha \cdot d_{cg-r}$	$\alpha \cdot d_{cg-r}$	ΣF_y
α	0	ΣM_r	ΣM_f	ΣM_{cg}
F_f	ΣM_r	$F_{f\,max}$	ΣF_y	$F_{f\,max}$
F_r	ΣM_f	ΣF_y	$F_{r\,max}$	$F_{r\,max}$

6. After calculating the lateral tire forces and lateral and angular accelerations assuming a particular lateral slip condition for the tires, it was necessary to determine whether the assumed tire slip conditions were still valid. The calculation to determine whether the tire slip condition had changed depended on the previous tire slip condition. If a set of tires were not slipping, then slippage would initiate when the calculated lateral tire force exceeded the maximum allowable value (eqs. 4a, b). If a set of tires were already slipping, then slippage would stop when its lateral velocity reached zero. Lateral tire velocities were obtained by first calculating the lateral accelerations of the vehicle at the center of the front (a_f) and rear (a_r) axles:

$$a_f = a_y + \alpha \cdot d_{cg-f} \qquad (6a)$$

$$a_r = a_y - \alpha \cdot d_{cg-r} \qquad (6b)$$

The lateral velocities of the front (v_f) and rear (v_r) tires were then calculated by numerically integrating the lateral accelerations. If the tire slip conditions were determined to have changed, it was necessary to repeat step 5 using a new set of governing equations determined by the new tire slip conditions (Table 1).

7. Next, all of the remaining parameters of interest describing the dynamics of the CG of each vehicle were calculated. The longitudinal acceleration (a_x) of the CG was calculated from Newton's second law. The linear velocity components (v_x and v_y) of the vehicle CG in the local vehicle coordinate frame were calculated by numerical integration of the acceleration components using the trapezoidal rule. Angular velocity and angular displacement were likewise calculated by integrating and double-integrating angular acceleration, respectively. The relative angle between the vehicles (θ) was then given by:

$$\theta = \theta_b - \theta_t \qquad (7)$$

To calculate linear displacements, the velocity vector for each vehicle was first coordinate transformed to the inertial frame:

$$\begin{bmatrix} v_x \\ v_y \end{bmatrix}_{inertial} = \begin{bmatrix} \cos\theta_{veh} & -\sin\theta_{veh} \\ \sin\theta_{veh} & \cos\theta_{veh} \end{bmatrix} \begin{bmatrix} v_x \\ v_y \end{bmatrix}_{veh} \qquad (8)$$

The position of the vehicle CG was then calculated by integrating the velocity vector for each direction in the inertial frame.

8. Once the calculations were complete, the data were output, the time was incremented, and steps 1 – 7 were repeated for the desired time duration.

VEHICLE CRASH TESTS

Experimental sideswipe collisions were staged with instrumented vehicles in order to validate the analytical model. A 1996 Ford Taurus was designated as the bullet vehicle and a 1996 Buick Skylark was designated as the target vehicle for all tests. The bullet vehicle was rolled at a predetermined velocity and approach angle into the side of the stationary target vehicle (Figure 1). Nominal closing speeds varied from 3 – 10 kph (2 – 6 mph) and all tests were conducted with an approach angle of 15° (Table 2). Both vehicles were placed in neutral and the steering wheel was fixed so that the tires were straight.

The bullet vehicle bumper was modified to accommodate load cells so that the inter-vehicular contact force could be measured directly. The front left corner of the Taurus bumper was cut away and reattached using a steel structure designed to recreate the original bumper configuration. The added structure allowed for two uniaxial 44 kN (10 kip) load cells (Model 1210AO, Interface, Inc.) to be placed in series between the cut-away bumper corner and the frame of the vehicle. The load cells were mounted at right angles to each other in order to measure both lateral and longitudinal forces.

This modification extended the profile of the bumper corner approximately 20 cm (8 in.) forward and 20 cm (8 in.) outboard of its original location (Figure 4). Accelerometers were mounted to the cut-away portion of the bumper corner to allow for mass compensation of the measured forces (Endevco 7290A-100-G). The right front corner of the bumper was left in its original and intact condition. In order to evaluate whether the bumper modification would alter the vehicle dynamics, matched tests were performed at identical approach speeds and angles on opposite sides of the vehicles. These matched tests comprised two test series, one in which the modified left front corner of the bullet vehicle struck the right side of the target vehicle (series M), and another in which the original right front corner of the bullet vehicle struck the left side of the target vehicle (series O).

Table 2. Vehicle test matrix. All tests were conducted at a 15° approach angle.

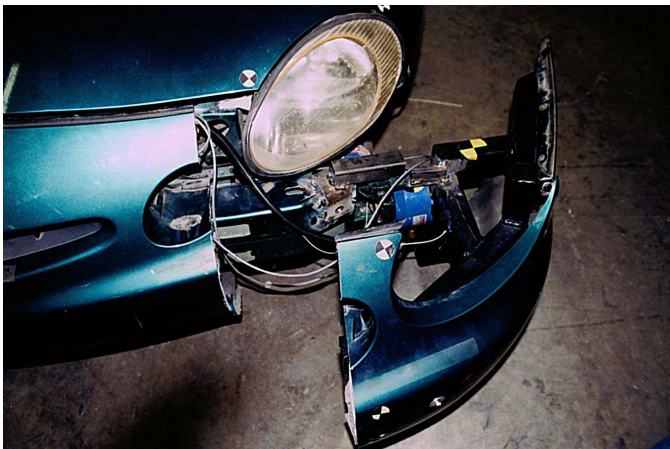| Test ID	Location of initial contact	Approach speed (kph)
M2	Front of rear door	3.4
M4	Middle of front door	6.4
M6	Middle of rear door	10.0
O2	Front of rear door	3.2
O3	Middle of front door	5.3
O4	Middle of front door	6.4
O6	Middle of rear door	9.5

Figure 4. Modified bumper corner on the 1996 Ford Taurus.

The approach speed of the bullet vehicle was measured using a Tapeswitch® speed trap. Both vehicles were instrumented with x-axis and y-axis accelerometers (Endevco 7596-10-G) mounted on the frame near the center of the front axle. A y-axis accelerometer (Endevco 7596-10-G) and z-axis angular rate sensor (ARS-01, ATA, Inc.) were mounted on the frame near the center of the rear axle (Figure 5).
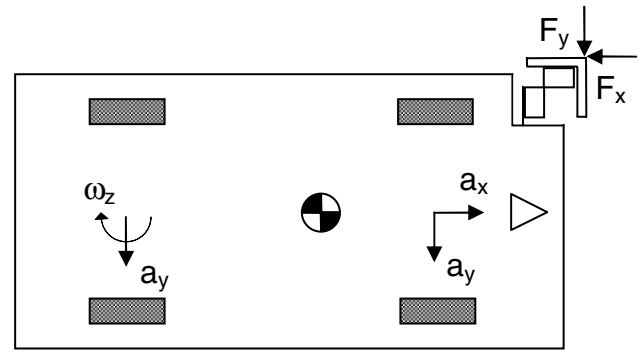

Figure 5. Schematic of vehicle instrumentation.

All data were sampled at 1 kHz using a 16-channel board (ISC-16E2, RC Electronics, Inc.) installed inside a PC connected to a 3-channel bridge conditioning and amplifying system (Model 136-1, Endevco Inc.). After acquisition, the data were debiased and filtered to 40 Hz. High speed (250 fps) video data were recorded from an overhead camera. Acceleration data were transformed to the SAE coordinate frame originating at the vehicle CG. Velocity data were obtained by integrating the acceleration data and also by differentiating displacement data acquired from digitized images of the high-speed video. Accelerometer data were debiased using the post-event offset, rather than the pre-trigger offset, because this method minimized the accumulated integration error and resulted in velocity time-histories that better matched the video data. Angular acceleration was calculated from the two y-axis accelerometers and integrated to obtain angular velocity. The coefficient of friction between the sliding surfaces of the vehicles was calculated using test data from the instrumented bumper. Bumper forces measured on the bullet vehicle were coordinate transformed to the target vehicle frame (eq. 3). The longitudinal target vehicle force was then plotted as a function of lateral target vehicle force, and a linear least-squares fit was performed. The slope of the line was taken as the inter-vehicular coefficient of friction μ_{slide}. The tire to ground coefficient of friction μ_{tire} was measured to be 0.6 by dragging the Ford Taurus laterally over the test area floor. This value was assumed for the Skylark, as well.

Post-test damage to both vehicles was carefully measured and documented in photographs. The length, height, and crush depth of the damaged area of the target vehicle were recorded, as was the width of the contact patch on the bumper of the bullet vehicle. Because multiple tests were performed on the same side of the target vehicle, the issue arose of how to distinguish the damage created by later tests from the damage left by earlier tests. This problem was addressed in later tests by coating the bumper of the bullet vehicle with a thin layer of face paint, the color of which was changed for every test. Video data were also utilized to determine the distance that the bullet bumper slid along the side of the target vehicle.

MODEL VALIDATION

Input parameters to the model were vehicle dimensions, masses, and inertial properties, as well as the coefficient of friction between the tire and the ground, the initial contact point on the side of the target vehicle, the approach angle and closing velocity of the bullet vehicle, the inter-vehicular sliding coefficient of friction, and the lumped lateral stiffness of both vehicles. All of these parameters were known beforehand or measured during the vehicle crash tests except for the lateral stiffness of the vehicles. This parameter was estimated by iteratively tuning the stiffness parameter until the model results matched the length of contact damage measured experimentally.

Computational modeling

The analytical model was used to iteratively solve for the optimal lateral stiffness value that matched a given output parameter in a specific vehicle test. The specific output parameter that was matched was the maximum inter-vehicular sliding distance of the bullet vehicle bumper on the side of the target vehicle. This corresponded to the length of the contact damage measured on the target vehicle minus the contact patch width on the bullet vehicle bumper [6]. In these simulations, the force-deflection relationship of the interacting vehicles was assumed to behave as a linear spring (eq. 1). The optimal spring stiffness k was obtained using an iterative solution procedure. An initial guess was made for k, and then this guess was increased or decreased in successive model simulations until the model output the desired inter-vehicular sliding length to within a predefined tolerance of 1 mm. This procedure was automated using a linear interpolation technique to update the guess for k until convergence was achieved.

The computational model was additionally used to study the relationship between closing speed, approach angle, and length of contact damage. When reconstructing a real world crash, the approach speed and angle of the bullet vehicle are unknown parameters. Therefore, a parametric analysis was conducted to examine the relationship between these parameters for each of the experimental tests. This was accomplished by again using an iterative solution procedure. For a given approach angle, the analytical model iteratively solved for the approach velocity required to create the measured sliding distance. This process was then repeated for a range of approach angles.

Quasistatic component tests

Quasistatic compression tests were performed on the contacting surfaces of two of the test vehicles in order to directly measure the lateral stiffness of the vehicles. Tests were performed on both the modified and original front bumper corners of the Taurus and at two points along the side of the Skylark. A hydraulic press was positioned horizontally at the same height, position, and angle at which sliding contact occurred in the vehicle tests. The contact surface of the press was a flat 15 cm x 15 cm (6" x 6") aluminum plate covered with a shop rag to prevent scraping of the vehicle surfaces. The press was instrumented with a load cell and displacement transducer. Tests were performed up to a lateral load level of approximately 3560 N (800 lbf.), which was not sufficient to cause lateral tire slippage. Lateral force-deflection curves were plotted for each vehicle surface. A combined force-deflection curve was generated for both vehicles in series by adding the vehicle deflections at each force level. This curve was compared to the linear stiffness parameter derived by tuning the model to match the length of contact damage in the experiments.

EDSMAC simulations

In order to compare our model results to existing methods, the four vehicle tests with the original bumper configuration (O series) were modeled using EDSMAC (version 2.51, 1993, Engineering Dynamics Corporation, Lake Oswego, OR). Where possible, the input parameters for the EDSMAC simulations were identical to the input parameters used in the analytical linear spring model. Stiffness parameters for EDSMAC were selected based on generic data for the class of passenger cars in the same wheelbase range as the subject vehicles [8]. For the bullet vehicle (Taurus), the frontal stiffness k_v was 93.4 lb/in^2. For the target vehicle (Skylark), the side stiffness k_v was 97.5 lb/in^2.

RESULTS

VEHICLE TESTS

The vehicle dynamics observed in the experimental sideswipe tests demonstrated consistent patterns. At the low closing speeds investigated in this study, the bullet and target vehicles tended to achieve a common velocity and stick together. Thus, little or no restitution was observed. No snagging was observed in this study. In all but the lowest speed tests, there was some lateral tire slippage of the bullet and/or target vehicle. When this occurred, the vehicles tended to rotate only a few degrees. During the collision, the target vehicle rolled on its suspension. This created a downward deflection in the contact damage as it progressed forward on the side of the target vehicle. In some of the lowest speed tests, the rebound of the suspension caused the vehicles to separate and actually end up traveling backward at the end of the test.

Accelerometer data collected during the sideswipe collisions staged in this study demonstrated long contact times (~ 1 s), low delta-V's (1.4 – 5.0 kph), low accelerations in the longitudinal direction (< 0.4 g's), even lower accelerations in the lateral direction (< 0.3 g's), and contact damage lengths ranging from 51 – 142 cm (20 – 56 in.) (Table 3). The contact patch width on the bullet vehicle bumper ranged from 10-20 cm (4 – 8 in.). The inter-vehicular sliding distance, equal to the length of the damage on the target vehicle minus the

contact patch width on the bullet vehicle bumper [6], ranged from 43 – 124 cm (17 – 49 in.). In some tests, inward pocketing of the bullet vehicle bumper was observed, but the bumper always popped back into its original shape after the test. No post-test deformation of the bumper was observed in any of the tests. Post-test door panel deformation on the target vehicle never exceeded 1 cm.

Table 3. Experimental results for the target vehicle.

Test ID	Δt (ms)	A_x (g's)	A_y (g's)	ΔV (kph)	Damage (cm)
M2	1000	0.11	-0.08	1.6	53
M4	870	0.21	-0.18	3.2	94
M6	900	0.38	-0.24	5.0	140
O2	830	0.10	0.08	1.4	51
O3	820	0.20	0.12	3.1	69
O4	1070	0.18	0.11	3.4	99
O6	1100	0.28	0.26	4.7	142

The forces applied to the front corner of the modified bullet vehicle bumper were measured in tests M2 and M4 (the load cells failed in test M6). The accelerations measured on the cut-away portion of the bumper tended to be very noisy and of low amplitude (1 – 2 g's). Because the cut-away portion of the bumper had a mass of only about 13.6 kg (30 lbf.), inertial compensation of the bumper load cell readings for the mass of the cut-away section was deemed unnecessary. The measured bumper loads were used to estimate the inter-vehicular sliding coefficient of friction. Tests M2 and M4 showed consistent results with respect to calculated target vehicle contact forces (Figure 6). The assumption of a constant coefficient of friction was validated by good linear fits to the data (R^2 = .74 in both tests). Based on the results of these tests (Table 4), an inter-vehicular friction coefficient of 0.5 was assumed in the analytical model.
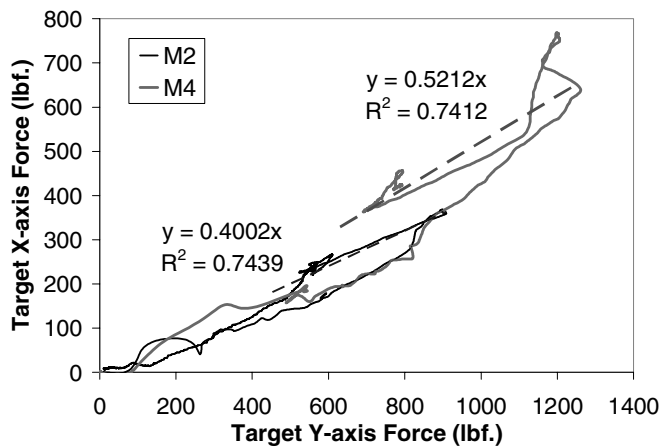

Figure 6. Estimate of the inter-vehicular coefficient of friction based on measured bumper loads.

Table 4. Data from tests with the instrumented bumper.

Test ID	Bullet Fx (lbf.)	Bullet Fy (lbf.)	Target Fx (lbf.)	Target Fy (lbf.)	μ_{slide}
M2	589	785	369	909	0.40
M4	1053	1053	769	1261	0.52

Acceleration data from tests with the modified bumper (series M) were very similar to acceleration data from matched tests conducted on the opposite side of the vehicles with the original bumper (series O) (Figure 7).
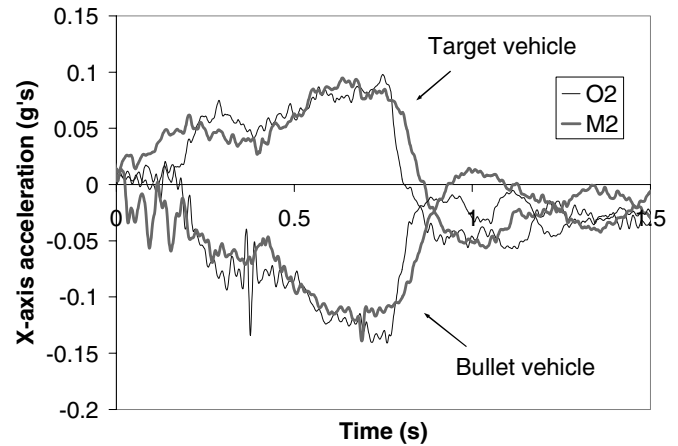

Figure 7. Matched tests comparing the original and modified bumper.

QUASISTATIC COMPONENT TESTS

The combined force-deflection properties of the Taurus bumper corner and the side of the Skylark were derived from the quasistatic lateral compression data of each vehicle (Figure 8). The combined stiffness of both structures in series showed progressive stiffening with increasing deflection. A quadratic equation was found to fit the data very well (R^2 = 0.99):

$$F_{yt}\left(lbf\right) = 15\frac{lbf}{in^2} \cdot d_{lat}^2\left(in\right) + 4.3\frac{lbf}{in} \cdot d_{lat}\left(in\right) \quad (9)$$
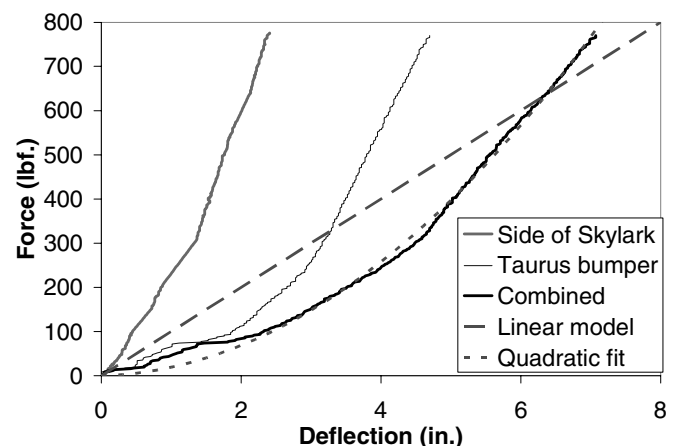

Figure 8. Quasistatic component test results.

MODEL VALIDATION

Optimal spring stiffness values for k were obtained for each test using the iterative solution procedure described previously. Optimal k values ranged from 100 – 115 lbf./in. with the exception of test O3, which had an optimized k value of 145 lbf./in. All of the experimental tests were modeled using both EDSMAC and a linear elastic spring model to define the force-deflection relationship between the vehicles. The linear spring model incorporated the optimized k value for each test such that the predicted length of contact damage matched the experimental data. The linear spring model also predicted no crush for any of the tests because it assumed full elastic rebound of the vehicle structures. EDSMAC, on the other hand, utilized generic crush-based stiffness parameters that were not optimized to match the damage observed experimentally. EDSMAC underpredicted the length of sliding contact damage by an average of 50% and overpredicted the amount of inward crush observed on the target vehicle (Table 5). However, the measurement of damage length provided by EDSMAC is somewhat coarse because the crush profile is given in polar coordinates spaced 3° apart. Therefore, the true error in damage length may be less than 50%.

Table 5. Comparison of vehicle damage measured experimentally and predicted by EDSMAC.

Test	Crush depth (in.)		Damage length (in.)	
	Exp	EDSMAC	Exp	EDSMAC
O2	0	1.6	20	16
O3	0	1.6	27	13
O4	<0.25	1.4	39	9
O6	~.25	2.3	56	26

The linear spring model matched the vehicle acceleration data (Figure 9) better than EDSMAC, which predicted a higher peak acceleration and shorter contact time than actually occurred. The average error between the predicted and measured peak target vehicle longitudinal accelerations was only 5% for the linear spring model (9% average absolute value of the error), compared to 83% for EDSMAC (Figure 10). Both the linear spring model and EDSMAC accurately predicted the vehicle delta-V's (Figure 11), which was expected because the initial velocities were given in both simulations. However, the linear spring model predicted the time it took for the vehicles to reach a common velocity more accurately than EDSMAC. The linear spring model also modeled the time course of the inter-vehicular force (Figure 12) with good accuracy. The linear model errors in estimating the peak lateral inter-vehicular force were 0.2% for test M2 and -4.5% for test M4.
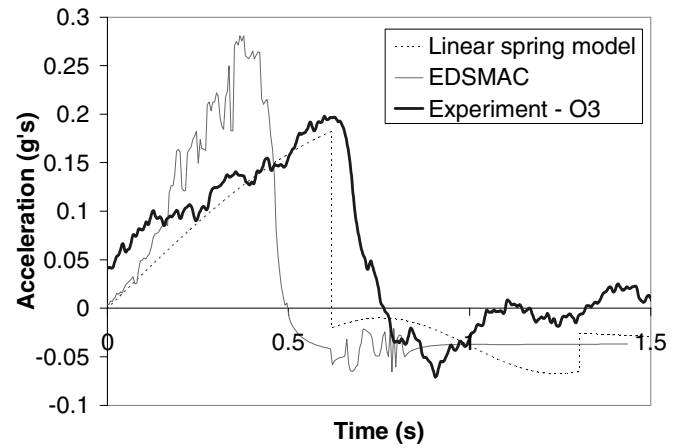

Figure 9. Comparison of model results, EDSMAC output, and experimental data for target vehicle x-axis acceleration in test O3.
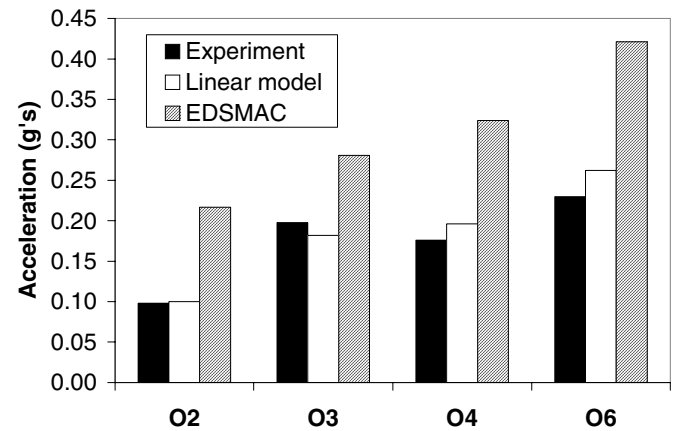

Figure 10. Comparison of model results, EDSMAC output, and experimental peak target vehicle x-axis accelerations measured in each test.
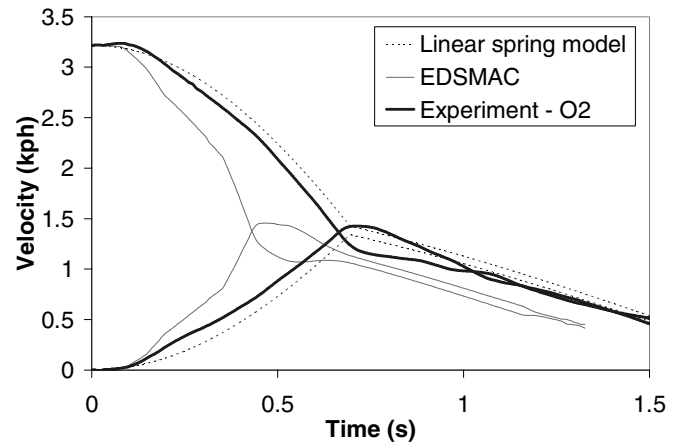

Figure 11. Comparison of model results, EDSMAC output, and experimental data for bullet and target vehicle velocities in test O2.

Although the linear spring model used a stiffness parameter that was tuned to match the experimental results, a sensitivity analysis demonstrated that the results of the model were not highly sensitive to the value of the lateral stiffness parameter k. An increase in stiffness from 100 lbf./in. to 150 lbf./in. generally increased peak accelerations and contact damage lengths by about 15%.
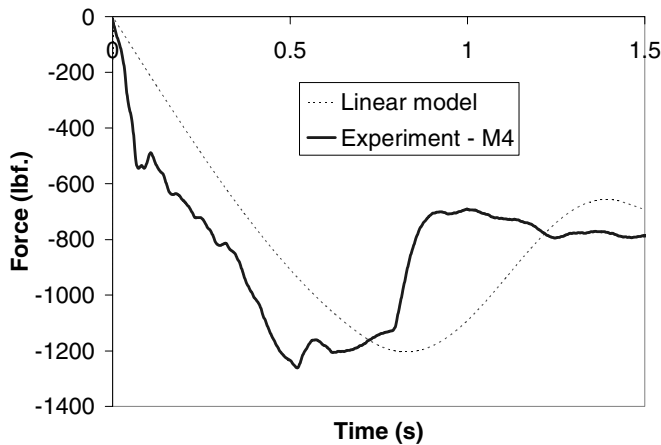
Figure 12. Comparison of model results and experimental data for lateral inter-vehicular force (Target vehicle Fy) in test M4.

A parametric analysis was performed using the analytical model to examine the sensitivity of the closing velocity estimation to the approach angle of the bullet vehicle. This analysis was performed for the experimental conditions of each test and demonstrated that the length of sliding contact damage did not uniquely determine the approach velocity of the bullet vehicle. The same damage length could be produced by a slow-moving bullet vehicle striking at a shallow approach angle as a faster-moving bullet vehicle approaching at a steeper angle. In fact, determination of the closing velocity was strongly dependent on the approach angle (Figure 13).
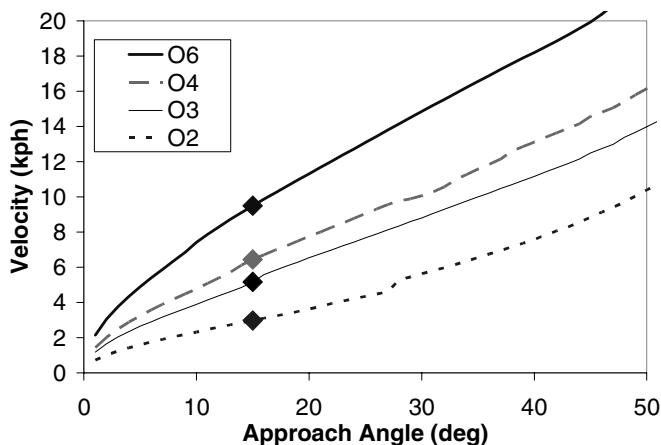

Figure 13. Sensitivity of the calculated closing velocity calculation to the approach angle. Model results are matched to the inter-vehicular sliding distance measured in each test (diamonds indicate a 15° approach angle).

DISCUSSION

ESTIMATION OF COLLISION SEVERITY

It is often the task of the crash investigator to reconstruct a collision in terms of engineering parameters that have some relationship to the injury potential posed to the vehicle occupants. In the case of a shallow angle sideswipe collision, the accelerations and changes in velocity are of a greater magnitude in the longitudinal direction than the lateral direction (Table 3). It has been reported that volunteers in vehicle crash tests tolerate

longitudinal accelerations better in frontal impacts than rear impacts [1]. Therefore, the engineering parameters of greatest interest in this study were the acceleration and velocity change experienced by the target vehicle in the longitudinal direction. The analytical model developed here predicted both the time course and the peak values of these parameters with excellent accuracy (Figures 9, 10, and 11).

It is notable that the vehicle dynamics of a sideswipe collision are markedly different from other types of collisions. The primary difference is that the contact duration in a sideswipe is very long (~ 1 s) compared to frontal, side, and rear impacts, all of which have collision durations in the 100 – 200 ms range [1]. Because the contact duration is approximately 5 to 10 times longer in a sideswipe than a rear impact, the peak vehicle acceleration may be on the order of 80% - 90% lower in a sideswipe than a rear impact having the same change in velocity. In addition, the vehicle's forward velocity develops over a much larger distance in sideswipe collisions compared to rear impacts due to the protracted contact duration. These differences in acceleration and contact duration become important when assessing collision severity and injury potential.

Collision severity is usually assessed in terms of the change in velocity, or delta-V, of the subject vehicle. Delta-V is a useful predictor of injury potential for two reasons. First, delta-V is directly related to the contact injury potential associated with a second collision resulting from an accumulated relative velocity that develops between a part of the occupant's body and the vehicle interior. Second, delta-V can often be used as a surrogate measure of vehicle acceleration when a pulse duration can be assumed. Vehicle acceleration may be useful in predicting non-contact injuries, such as "whiplash" neck injuries. This injury mechanism is of particular concern in rear impacts and sideswipes in which one of the vehicles is accelerated forward. Because a normally seated occupant has his or her torso against the seat back, the magnitude of the vehicle's forward acceleration has a profound influence on the motion of the torso with respect to the head. Numerous investigators have shown that for a rear impact of a given delta-V, injury potential increases at higher levels of vehicle acceleration [9-11]. This phenomenon suggests that for a given velocity change, the injury potential in a sideswipe collision might be far lower than for a rear impact having a comparable velocity change. It is therefore valuable to use a model such as EDSMAC or the one proposed here so that vehicle acceleration can be modeled and considered along with delta-V as an additional indicator of injury potential.

MODEL PARAMETERS

Inter-vehicular coefficient of friction

A key assumption in the model is that longitudinal interaction between the vehicles is purely frictional. The use of an instrumented bumper allowed for a direct

measurement of the inter-vehicular coefficient of friction. To our knowledge, the coefficient of friction between sliding vehicle contact surfaces has never been measured in a dynamic vehicle test. The limited data from the current study support the assumption that the longitudinal force was linearly related to the lateral force (Figure 6). There was concern that the face paint applied to the vehicle surfaces may have affected the coefficient of friction. However, sliding distance was not significantly different in matched tests with (O2 and O4) and without (M2 and M4) the paint (Table 3). Calculated values for μ_{slide} in the present study were within the range of friction coefficients generally reported in the literature, but were slightly lower than the 0.6 coefficient of friction assumed by Toor et al. [6].

Lateral inter-vehicular stiffness

One difficulty in applying this model to real world collisions is that the lateral force-deflection relationship for two colliding vehicles is not known a priori. Existing vehicle side stiffness data are generally meant to characterize the crush properties of the vehicle in high speed collisions. However, when modeling sideswipes, it is desired to characterize the lateral stiffness of the vehicle at much lower impact forces. At low forces, the overall side compliance of the vehicle is dominated by lateral motion of the suspension and tire sidewalls, rather than permanent crush of the door and body panels. The quasistatic component tests were conducted in an effort to measure this lateral stiffness at low levels of force without any crush.

It was interesting to note that the simple linear model provided an excellent fit to the experimental data. One limitation of this single degree-of-freedom model was that it assumed that the vehicle did not accelerate laterally unless there was lateral tire slippage. However, real vehicles are sprung masses with lateral compliance between the tires and vehicle body due to suspension and tire sidewall stiffness. Therefore, it would probably be more accurate to model the lateral vehicle interaction as a two degree-of-freedom system. In a two degree-of-freedom model, the lateral inter-vehicular force in a dynamic sideswipe collision would be higher early in the event due to the lateral acceleration of the vehicle body that would occur prior to lateral tire slippage. Indeed, the experimental data exhibited higher contact forces and vehicle accelerations than were predicted by the model early in the event (Figures 10 and 13). Later in the event, the lateral inter-vehicluar force may be lower in a two degree-of-freedom model than a single degree-of-freedom model, depending on the vibrational characteristics of the system. Development of a two degree-of-freedom model was not undertaken in the current study because it appeared that the much simpler one degree-of-freedom linear spring model accurately captured the desired longitudinal behavior over a range of test speeds. The optimized k values calculated by the model were remarkably consistent for each test, which suggests that this parameter is not sensitive to impact speed over the range studied. It was interesting to note

that the tuned k values approximated a linear fit to the quasistatically measured combined force-deflection data over the force range experienced during the vehicle tests (Figure 8).

In the current study, the lateral inter-vehicular stiffness properties of a Ford Taurus bumper corner striking the side of a Buick Skylark have been explored in some detail. Unfortunately, this parameter is not known for other combinations of vehicles that may become involved in real world sideswipe collisions. More testing on different types of vehicles is necessary before generic values of the lateral inter-vehicular stiffness can be established for general use with the analytical model presented here. In addition, the current model is most applicable to situations with no crush because it assumes an elastic linear spring. Adding hysteresis to the model may improve its performance in predicting crush depth in more severe collisions.

Tire slippage

Tire forces are typically ignored in high speed crashes because their magnitude is much smaller than the inter-vehicular contact force. For low speed frontal, side, and rear impacts, tire forces can be effectively modeled by assuming a constant braking or sliding force during the crash pulse. However, for sideswipe collisions, the crash pulse is very long, and tire forces and slip conditions may change appreciably during the event. In fact, the sideswipe may be the only type of collision for which it is essential to keep track of the changing lateral tire forces and slip conditions during the crash pulse in order to accurately model the collision dynamics. This is due to the large number of governing equations that are dependent on the model keeping track of which tires are slipping laterally (Table 1). It is worth noting that the equations governing whether the lateral tire slip conditions have changed are themselves dependent on the lateral slip condition of the tires. Thus, the equations of motion in the model had to be formulated as an initial value problem in which it was known that no tires were slipping laterally prior to the initiation of vehicle contact. It was found that lateral tire slip conditions sometimes changed several times during the collision, resulting in discontinuities in calculated accelerations (Figure 9). Discontinuities in acceleration are physically realistic and occur when sliding stops, either between the tires and the ground, or between the vehicle contact surfaces.

SPEED-ANGLE RELATIONSHIP TO DAMAGE

It would be desirable to be able to reconstruct sideswipe collisions based solely on observed vehicle damage, as is often possible for other types of collisions. However, results from the model suggest that the same length of contact damage may be produced by a family of crash configurations of widely varying closing speeds and approach angles (Figure 13). This phenomenon was not verified experimentally in this test series, however. For a given length of contact damage, the associated vehicle dynamics would vary considerably depending on the

combination of closing speed and approach angle. It is therefore impossible to determine a pre-impact speed for the bullet vehicle without knowing or assuming an approach angle. This presents a serious difficulty to the crash investigator analyzing real world sideswipe collisions. In some cases, it may be possible to estimate the approach angle or closing speed based on witness statements, scene geometry, crush pattern, or other information.

The analytical method proposed by Toor et al. [6] does not recognize the interrelationship between closing speed and approach angle to post-crash vehicle damage. This flaw in their method is a consequence of using vehicle side stiffness coefficients to calculate the lateral inter-vehicular force. Because the method is intended for use in cases of little or no crush, the calculated force is essentially the "A" stiffness coefficient multiplied by the width of the contact patch measured on the bullet vehicle bumper. Not only is this method highly sensitive to the contact patch width on the bumper of the bullet vehicle, which may be difficult to measure, it also has the effect of fixing the lateral inter-vehicular force to a constant and unchanging force level, regardless of the closing speed or impact angle of the bullet vehicle. Data from the instrumented bumper test series in this study demonstrate that the inter-vehicular force changes during the collision (Figure 12) and that its peak value increases with increasing impact speed (Table 4). It is difficult to determine the approach angle in the tests conducted by Toor et al. [6], because in their test configuration, a moving target vehicle strikes a stationary bullet vehicle. This was accomplished by steering the target vehicle into the bullet vehicle, which violated the stated assumption that all tires were steered straight. The steering angle in the Tooret al. study corresponds roughly to the approach angle in the current study, and therefore its magnitude would have substantially influenced the length of contact damage in the tests.

COMPARISON TO EXISTING MODELS

The linear spring model developed in this study calculates vehicle motions using a method similar to SMAC, but with a novel method of calculating inter-vehicular forces. Most existing accident reconstruction algorithms, such as SMAC, CRASH, IMPAC, and the method of Toor et al. use crush-based stiffness coefficients to calculate inter-vehicular forces. This method is well-validated for a wide variety of moderate and high-speed collisions and makes use of the extensive crash test data that is publicly available. Unfortunately, the accuracy of a crush-based method will necessarily degrade in cases where crush is low or nonexistent. In these cases, specialized methods have to be developed, such as examination of bumper isolator compression in low speed rear impacts [1]. The current model is similarly a specialized method of calculating lateral inter-vehicular force in a sideswipe collision using an elastic linear stiffness model meant to characterize the combined lateral stiffness of both vehicles before significant crush develops. Longitudinal force is treated

as frictional contact, which is not a novel approach and is used in all of the algorithms mentioned above.

Of all commonly used existing methods, EDSMAC was deemed the most appropriate for comparison with the current model. Like the current model, EDSMAC is a simulation that provides vehicle acceleration time histories as a primary output in addition to delta-V. The experimental data presented here suggest that EDSMAC, when run with generic stiffness coefficients, does not accurately model low speed sideswipe collisions. It should be noted that EDSMAC's overestimation of vehicle acceleration and underestimation of damage length are additive. If EDSMAC were run iteratively to find the collision velocity that matched the observed length of contact damage, then the collision velocity would be substantially overestimated, which would in turn exacerbate the overestimation of the vehicle accelerations. These data suggest that generic stiffness coefficients overpredict the stiffness characteristics of vehicles in low speed sideswipe collisions.

It may be possible to modify SMAC to more realistically model low speed sideswipe collisions. It would certainly be necessary to reduce the stiffness coefficients compared to their generic values. One approach would be to optimize the stiffness coefficients for these types of crashes based on experimental data, and then relate these optimized values to the generic values. However, decreasing the stiffness coefficients would increase the predicted crush depth. This parameter would have to be interpreted as dynamic displacement rather than residual damage. It should be noted that the stiffness coefficients presented in this paper are not directly comparable to the generic stiffness coefficients used by SMAC, because our model calculates lateral inter-vehicular force differently than SMAC does. SMAC calculates force based on the area of vehicle overlap, whereas our model only considers the lateral overlap distance. The SMAC model progressively stiffens with lateral overlap distance due to the corresponding increase in longitudinal overlap. Our model, on the other hand, assumes a constant stiffness regardless of the amount of longitudinal overlap. This difference could be reduced somewhat by using rounded bumper corners in the SMAC model.

In defense of SMAC, it has many well-developed and useful features that our model lacks, such as a detailed tire model that incorporates braking, steering, cornering stiffness, and slip-angle saturation. The tire model used in the current study is quite rudimentary. All of the governing equations were formulated assuming the tires were steered straight and free rolling, with lateral slip governed by Coulomb friction. This simplified tire model was deemed sufficient for modeling our experimental tests, but would be of limited value in other impact situations. The situation could possibly be remedied by adding a more detailed tire model to our model. A more attractive alternative would be to modify SMAC to incorporate our linear spring method of calculating inter-vehicular forces for the specialized case of sideswipe collisions with low levels of crush.

CONCLUSIONS

An analytical model based on the equations of motion of a linear spring-mass system was developed to investigate the vehicle dynamics of sideswipe collisions and implemented as a FORTRAN program. The model was similar to the SMAC algorithm, but incorporated a novel non-crush-based method of calculating inter-vehicular forces based on vehicle overlap and frictional contact. Staged sideswipe crash tests were performed with instrumented vehicles and the results were compared to the linear spring model and EDSMAC. The linear spring model accurately predicted the time course and peak values of the vehicle accelerations and velocities measured in the experimental tests. EDSMAC substantially overpredicted vehicle accelerations and underpredicted the length of contact damage measured in the experimental tests. These results demonstrate that an optimized characterization of lateral vehicular stiffness below the crush threshold was more accurate than using generic stiffness coefficients to calculate inter-vehicular forces in these experimental sideswipe collisions. The experimental results show that at velocity changes of 5 kph or less, sideswipe collisions are characterized by very long contact durations (~1 s) and very low vehicle accelerations (< 0.4 g's). Therefore, a shallow angle sideswipe collision would be expected to pose a lower risk of injury to a vehicle occupant than a rear impact having a comparable velocity change. The analytical model developed here also demonstrated that it is not possible to fully reconstruct a sideswipe collision based on observations of vehicle damage alone.

ACKNOWLEDGMENTS

REFERENCES

1. Bailey, M.N., Wong, B.C., Lawrence, J.M., "Data and Methods for Estimating the Severity of Minor Impacts," 950352, Society of Automotive Engineers, Warrendale, PA, 1995.
2. Levy, R.A., "Speed Determination in Car-Truck Sideswipe Collisions," 2000-01-0463, Society of Automotive Engineers, Warrendale, PA, 2000.
3. Woolley, R.L., "The 'IMPAC' Computer Program for Accident Reconstruction," 850254, Society of Automotive Engineers, Warrendale, PA, 1985.
4. McHenry, R.R., "Computer Program for Reconstruction of Highway Accidents," 730980, 17th Stapp, 1973.
5. Fonda, A.G., "CRASH Extended for Desk and Handheld Computers," 870044, Society of Automotive Engineers, Warrendale, PA, 1987.
6. Toor, A., Roenitz, E., Johal, R., Overgaard, R., Happer, A., Araszewski, M., "Practical Analysis Technique for Quantifying Sideswipe Collisions," 1999-01-0094, Society of Automotive Engineers, Warrendale, PA, 1999.
7. Prasad, A.K., "Energy Absorbed by Vehicle Structures in Side-Impacts," 910599, Society of Automotive Engineers, Warrendale, PA, 1991.
8. Siddall, D.E. and Day, T.D., "Updating the Vehicle Class Categories," 960897, Society of Automotive Engineers, Warrendale, PA, 1996.
9. Krafft, M., "Influence of Velocity Change and Car Acceleration on Short- and Long-Term Disability Risk in Rear Impact," in Frontiers in Whiplash Trauma, ed. N. Yoganandan and F. Pintar, IOS Press, 2001.
10. Jakobsson, L., Norin, H., Jernstrom, C., Svensson, S., Johnsen, P., Isaksson-Hellman, I., Svensson, M.Y., "Analysis of Different Head and Neck Responses in Rear-End Car Collisions Using a New Human-like Mathematical Model," *Proc. International IRCOBI Conf.*, pp. 109-126, 1994.
11. Olsson, I., Bunketorp, O., Carlsson, G., Gustafsson, C., Planath, I., Norin, H., Ysander, L., "An In-Depth Study of Neck Injuries in Rear-End Collisions," *Proc. International IRCOBI Conf.*, pp. 269-282, 1998.

CONTACT

James R. Funk, Ph.D., is a biomechanical engineer employed by Biodynamic Research Corporation in San Antonio, TX. Please direct any questions or comments regarding this paper to:

James R. Funk
Biodynamic Research Corporation
5711 University Heights Blvd., Suite 100
San Antonio, TX 78249
Phone: 210-691-0281
Fax: 210-691-8823
E-mail: jfunk@brconline.com